Pergamon

Carbon Vol. 0, No. 5, pp. 0–0, 1995

0008-6223/95 $9.50 + 0.00

0008-6223(95)00000-0

SOLVENT CLEANSING OF THE SURFACE OF CARBON FILAMENTS AND ITS BENEFIT TO THE ELECTROCHEMICAL BEHAVIOR

XIAOPING SHUI,[1] C. A. FRYSZ[2] and D. D. L. CHUNG[1]
[1]Composite Materials Research Laboratory, Furnas Hall, State University of New York at Buffalo, Buffalo, NY 14260-4400, U.S.A.
[2]Wilson Greatbatch Ltd., 10000 Wehrle Drive, Clarence, NY 14031, U.S.A.

(*Received* 7 *April* 1995; *accepted in revised form* 12 *June* 1995)

Abstract—The surface of vapor-grown carbon filaments (types H79 and ADNH of Applied Sciences Inc.) was found to be covered with a layer of tarry substance (comprising primarily polyaromatic hydrocarbons and originating from the filament growth process), which degraded the electrochemical performance (as shown by cyclic voltammetry using the $Fe(CN)_6^{-3/-4}$ redox couple), increased the filament-to-filament electrical contact resistivity in a binderless filament compact and decreased the filaments' compactability. Solvent cleansing removed the tarry coating, thereby exposing oxygen-containing functional groups. The coating was more tenacious on H79 than ADNH filaments. For ADNH, either acetone or methylene chloride cleansing removed the coating; for H79, methylene chloride cleansing removed the coating, but acetone cleansing did not. Chopping the cleansed filaments in a liquid medium using a blender helped maintain ADNH filament compaction after pressure release, thereby further improving the electrochemical performance, though it was not necessary for H79. Cleansing and chopping raised the electron transfer rate constant (k_s) of ADNH by up to 500%, so that k_s up to 0.02 cm/s was attained, and decreased capacitance and electrochemical area. For H79, cleansing removed the high residual current density, but degraded the rate constant by up to 70%. Graphitization decreased the electrical resistivity and increased the compactability of ADNH, but degraded the electrochemical performance because of a change in surface functional groups. In contrast to conventional carbon paste electrodes, carbon filament compacts, if not graphitized, did not require any binder.

Key Words—Carbon filaments, carbon fibers, vapor-grown, electrochemical, voltammetry, surface treatment, graphitization, acetone, methylene chloride.

1. INTRODUCTION

Various carbon materials are known to deposit during the thermal processing of carbonaceous gases. Their structures are generally grouped into three categories: amorphous carbon, well ordered graphitic platelets and filamentous carbon[1–5]. Recently, considerable interest has been directed toward using the last of the three groups (specifically, vapor-grown carbon filaments) for electrochemical applications such as electrodes. Carbon filaments are small in diameter (typically less than 1 μm), which results in a rather large surface area, an important characteristic for electrode applications. In addition, unlike particles, carbon filaments tend to cling to each other. This tendency allows shapeability without the need for binders or oils. Although not yet widely produced, carbon filaments are potentially one of the primary carbon materials for electrochemical applications.

The growth of carbon filaments involves a catalyst, usually a Group VIII metal. Iron and nickel are exceptionally good for catalyzing filament growth[2]. This was realized when carbon deposits forming inside stainless-steel hydroprocessing equipment in chemical plants were analyzed, and when coke steam reforming catalysts were examined. Because of the deleterious effects of the deposited carbon inside the reactor tubes and in catalyst coking, the carbon filament growth process was extensively studied[6–10]. In general, the source gas is carbon monoxide or many different hydrocarbons. Methane and other aliphatics, olefins and aromatics also produce carbon filaments when exposed to the appropriate catalysts[11–17]. The rate of filament growth can be reduced or stopped if gases which are able to gasify carbon are present (for example, hydrogen, carbon dioxide or water vapor).

Carbon filaments differ from conventional carbon fibers and whiskers in their fabrication process, and from the fibers in their size. Conventional carbon fibers are typically prepared either from a pitch material or from a polymer precursor such as polyacrylonitrile, and whiskers are characteristically formed during the pyrolysis of hydrocarbons. Both processes lack a catalyst. Regarding size, the filaments (like whiskers) have diameters (that are typically $\sim$0.1 μm). The diameter of conventional carbon fibers, on the other hand, is typically 10 μm. Two characteristics important to electrochemical applications are shared by the fibers, the whiskers and the filaments: a high geometric aspect ratio and high electrical conductivity.

Carbon filaments also differ from vapor-grown carbon fibers as developed by Tibbetts and co-workers[18–20]. Vapor-grown fibers begin as carbon filaments, but the conditions of the process

carbon0385 27-09-95 15:40:09 Rev. 10*PS
The Charlesworth Group, Huddersfield 01484 517077

are such that, in addition to the catalytic filament formation, non-catalytic carbon deposition occurs. This deposition takes place on the outside of the carbon filament causing it to grow radially, so that the final product has dimensions that are characteristic of a conventional carbon fiber. Temperature is the primary variable that determines whether a catalytic filament or a vapor-grown fiber is produced.

Two types of filament, H79 and ADNH, supplied by Applied Sciences Inc. (Cedarville, Ohio) were used in this study. Both types of filament were made using methane as the primary source gas and an iron-containing catalyst. Hydrogen sulfide was added to the feedstock in small amounts to increase filament yield[21]. It has been reported that the sulfur addition causes the iron to melt and encourages filament growth by the vapor–liquid–solid process, as hydrocarbons adhere better to molten particles and carbon atoms may diffuse more rapidly through molten particles[22]. The H79 was grown without ammonia gas in the feedstock (in contrast to ADNH) and at a lower temperature compared to that used for ADNH. Flowing air was used to harvest the filaments from the growing chamber, less being used to harvest H79 filaments than to harvest ADNH filaments. Because of the differences between these processes, Applied Sciences speculates that the H79 filaments have more contamination on the surface than the ADNH, and furthermore, that the contamination is a soot rather than a tarry material. The H79 is also thought to have less oxygen and nitrogen on the surface in comparison to ADNH[21].

Since much knowledge relative to the production process has been gained, current research efforts focus on potential applications for carbon filaments. The primary effort has been focused on structural applications, such as the replacement of carbon black in the manufacture of tires or their use as the reinforcement in composites. Investigations that focus on electrode applications, for example battery electrodes, are in their infancy[23–25]. Studies are needed of filament electrochemical performance. Since very little work has been conducted using cyclic voltammetry (CV), and since CV is a good way to assess electrode reaction kinetics and to compare materials and material surface treatments, this research was initiated.

The kinetics and reversibility of electrochemical processes depend strongly on the surface of the electrodes. Therefore, surface treatments are commonly applied to electrode materials, including changes in the surface functional groups, surface crystallographic structure and surface roughness. They may involve chemical treatment, heat treatment, laser treatment, plasma treatment, polishing or other surface activation. In particular, in the case of carbon materials, acid treatment[26–31], heat treatment[32,33], laser treatment[34,35] and electrode polishing procedures[36] have been employed. These treatments tend to increase the oxygen-containing functional groups on the surface of the carbon. In the case of high temperature heat treatment in an inert or reducing atmosphere or *in vacuo*, graphitization of the carbon can take place, thus changing the crystallographic structure both in the surface and in the bulk. Heat treatment in the presence of oxygen causes oxidation, thus increasing the amount of oxygen-containing functional groups on the surface and even converting the carbon to CO or CO_2 gases (thereby roughening the surface).

In contrast to the surface modifications mentioned above, this paper involves surface cleansing, which removes undesirable materials from the surface through washing in a solvent. Cleansing has not previously been applied to carbons, but in this work it was found to greatly improve the electrochemical behavior of vapor-grown carbon filaments (consistently increasing the electrode rate constant of ADNH as high as 0.02 cm/s) owing to the fact that a tarry residue remains on the surface of these filaments after the filament growth process, which involves a carbonaceous gas. An objective of this paper is to study the process and effect of the cleansing of carbon filaments. A related objective is to compare the effect of cleansing with the effect of graphitization heat treatment.

For electrochemical applications such as battery and analytical electrodes or capacitors, electrode capacitance is as important a parameter to performance as electrode kinetics. In the former, it is desirable to have a low capacitance in conjunction with a high electron transfer rate. In the latter, a high capacitance and a high electron transfer rate is sought. High capacitance is often associated with high surface roughness or high concentration of oxygen-containing surface functional groups, whereas low capacitance is usually due to poor wetting by the electrolyte[37]. Slow capacitive charging has been shown to occur when the electrode displays limited conductivity or exhibits an inhomogeneous surface[37].

A carbon electrode for analytical or battery applications is in the form of a bulk solid (e.g. pyrolytic graphite and glassy carbon), carbon fibers (typically 10 μm in diameter and made from pitch or polymers rather than carbonaceous gases) or an agglomerate of carbon particles (e.g. graphite particles and carbon black). The agglomerate form is most common in practice because of its formability and low cost. The agglomerate can be a dry compact or a paste (containing a binder such as an oil or wax). Since electrical conduction is required in the electrode, a low electrical resistivity is desirable. In the case of an electrode in the agglomerate form, the electrode's resistivity is governed by the volume resistivity of the individual units in the agglomerate as well as the contact resistivity between adjacent units. The contact resistivity is affected by the surface condition of the units. However, no previous work has been performed to study the effect of the surface condition on the contact resistivity. An objective of this paper is to study this effect in the case of the units being vapor-grown

carbon filaments and the agglomerate having no binder.

In the case of an electrode in the form of an agglomerate, the degree of compaction affects the electrochemical behavior of the electrode. A high degree of compaction is desirable, as it decreases the contact resistivity between the filaments and increases the amount of electrochemically active material per unit area of the outer surface of the electrode. As a result of the importance of the degree of compaction, the compactability of the units affects electrode performance. In general, filaments are harder to compact than particles and the compactability increases with decreasing filament length. The poor compactability of filaments is due to the tendency for the filament compact to spring back partially after pressure release. Therefore, an objective of this paper is to characterize and improve the compactability of the carbon filaments after pressure release. For this purpose, both compactability at pressure and compactability after pressure release were addressed in relation to the effect of filament treatments.

2. EXPERIMENTAL

Applied Sciences Inc. supplied two types of carbon filament with lengths greater than 100 μm: (i) ADNH of filament diameter 1500 Å, and (ii) H79 of filament diameter 500 Å. Initial studies were conducted on the as-received filaments, wherein it was noted that their surfaces were coated with a sticky residue. Removal of the residue was carried out using reagent grade acetone or reagent grade methylene chloride. To cleanse, the filaments were immersed in the solvent and stirred for 10 minutes using a Fisher Scientific Model 210T stirring plate. This caused the solvent to change from clear to dark, indicating the cleansing action of the medium. The filaments were separated from the solvent by pouring the mixture through filter paper. This was repeated four times or until the solvent remained clear. After filtration, the cleansed filaments were allowed to air dry in a low-humidity environment (< 1% relative humidity) overnight or in an oven at 140°C for a minimum of 6 hours before testing.

To determine the constituents of the residue removed by solvent cleansing, the filtrate was evaluated using a Mattson Cygnus 100 Fourier transform infrared spectrometer (FTIR) in conjunction with the ICON v1.2f software on a Dell 316sx personal computer. The decanted acetone and methylene chloride of the first wash were individually placed between two sodium chloride salt plates and evaluated in the transmission mode. The data were collected over 16 wave number scans from 500 to 4000 cm^{-1} at a wave number resolution of 4 cm^{-1}.

To determine the molecular structure of the material removed during solvent cleansing, gas chromatography/mass spectroscopy (GC/MS) was conducted by using a Hewlett-Packard 5970 MSD equipped with a 5890 GC. The solvent filtrates were concentrated by evaporating the cleansing medium prior to analysis. The gas chromatograph column was a 15 meter DB-5 fused silica capillary. The concentrated filtrate (1 μl) was injected into the column, held at 50°C for 3 minutes, then heated at 10°C/min to a final temperature of 290°C. The mass spectrometer was operated in the electron impact mode and the sample was scanned from 35 to 550 atomic mass units. The sample spectra were compared to the library spectra to identify components.

The effect of solvent cleansing on the filament surface composition was evaluated using electron spectroscopy for chemical analysis (ESCA), a high-vacuum surface science technique. (ESCA was performed only on the as-received ADNH, the ADNH cleansed with acetone and that cleansed with methylene chloride, in order to gather data relative to the effects of the treatments on the filament surface character.) The Small Spot ESCA, Model SSX100 from Surface Sciences Labs, was operated in the surface survey scan mode (i.e. without depth profiling) with a spot size of 600 μm. ESCA analysis was also performed after lightly sputter etching to a depth of 20 Å (with respect to silicon dioxide, which was used for depth calibration) to eliminate adventitious carbon.

To assess the impact of crystallinity on the electrochemical performance of the carbon filaments, an ADNH carbon filament sample was sent to St. Mary's Carbon Co. (St. Mary's, Pennsylvania) for graphitization at 2600°C. The filaments were placed on a graphite sagger and packed on all sides in graphitized charcoal to a depth of approximately 1 inch. The graphitized charcoal was then surrounded by an additional layer of ungraphitized charcoal. The self-generating atmosphere (produced by the volatization of the packing charcoals) protected the load from oxidation by air. Current was passed through the graphite sagger at a rate of 8 kW/lb, thus heating the load to the graphitization temperature after approximately 32 hours. The load was held at the graphitization temperature for 10–12 hours. The power was disconnected and the filaments were allowed to cool to room temperature, a slow process requiring 3–4 days.

Transmission electron microscope (TEM) bright field images were obtained for the as-received ADNH and H79 filaments using a Hitachi TEM, Model 100 CX, operated at 100 kV. In addition, electron diffraction was conducted on the as-received and graphitized versions of the ADNH filaments in order to compare the preferred orientation of their crystalline planes relative to the filament cylindrical surface before and after graphitization. The sample grid was immersed in a suspension of the filaments in Formvar® (ethylene dichloride in a 0.25% solution from Tousimis Research Corp.). Upon removal, a thin, electron-transparent film of evenly distributed filaments formed and dried on the grid. Electron diffraction conducted on the H79 filaments gave a multi-filament polycrystalline pattern, as the small size of the H79

filaments precluded individual filament crystallographic analysis. The larger size of the ADNH filaments made a single filament diffraction pattern possible. X-ray diffraction (Cu Ka radiation) was conducted to examine the crystallographic nature of the as-received carbon filaments and of the graphitized filaments. The intensities and widths of the 002 graphite peak (the only peak observed) for the various samples were compared.

As a result of the small diameter of the carbon filaments, single filament electrical resistivity measurement was impossible. Thus, the variation of the electrical resistivity of the carbon filament compacts (under pressure) with the filament type, filament treatment and compacting pressure was investigated. The compacting pressure is directly proportional to the contact pressure for a given filament geometry. It is well-known that the contact resistivity decreases with increasing contact pressure for electrical contacts in general. The four-point probe method pioneered by Wenner in 1916 was used[38]. The testing fixture is shown in Fig. 1. The design incorporates a bar-shaped cavity into which the carbon filaments were placed and compacted (without any binder) using a piston at a controlled pressure. Secured to the ends of the mold were probes used to pass current. Attached to the fixture insert bar were two more probes placed a known distance (l) apart. The potential developed across these two probes was measured as current was passed through the end probes. The material electrical resistivity (ρ) was determined as a function of the applied pressure from l, the cross-sectional area of the sample, A, and the potential drop, ΔV, between the probes for a known current flow, I, through the bar, using eqn (1).

$$\rho = (\Delta V/I)(A/l) \quad (1)$$

Filament electrochemical performance was assessed by cyclic voltammetry (CV). A Bioanalytical Systems (BAS) CV cell was used (Fig. 2) along with the Head Start electrochemistry software developed by EG&G Princeton Applied Research, a potentiostat and an IBM personal computer. The test solution in CV comprised 6 mM potassium ferricyanide (or potassium hexacyanoferrite (III) in IUPAC nomenclature) ($K_3Fe(CN)_6$), the electroactive species, in 1 M potas-

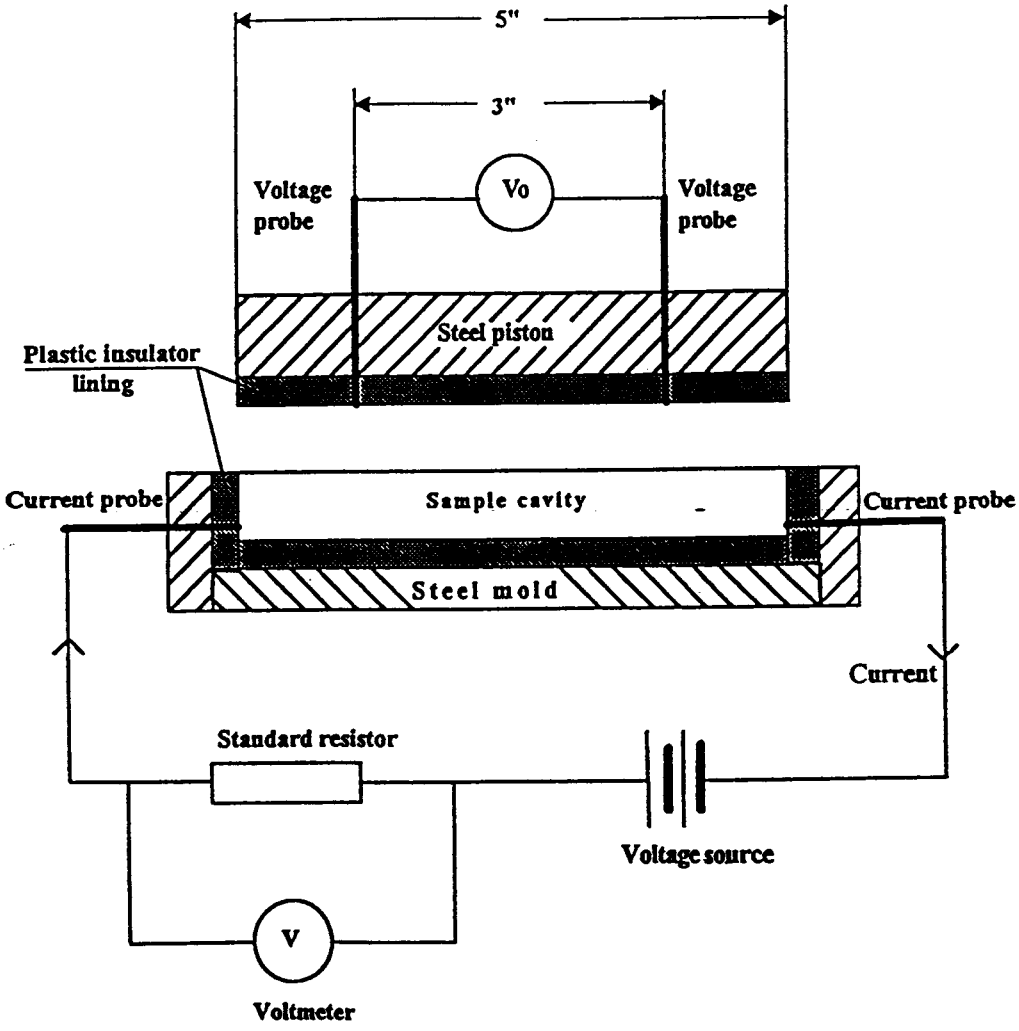

Fig. 1. Set-up for the four-point probe method for measuring electrical resistivity of filament compacts.

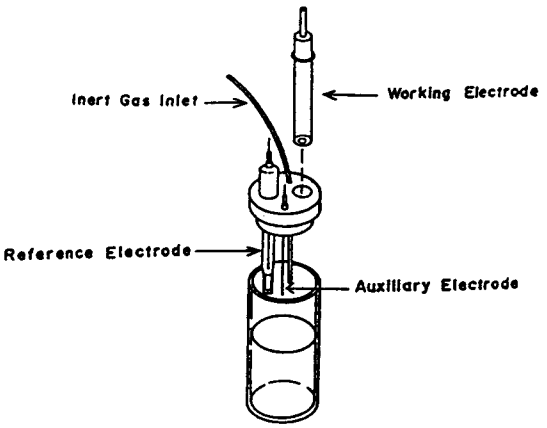

Fig. 2. Cyclic voltammetry cell from Bioanalytical Systems.

sium nitrate [KNO_3] in water, the supporting electrolyte. The solution was purged with argon prior to electrochemical testing through a gas inlet tube. A saturated calomel electrode served as the reference and a platinum wire as the auxiliary electrode. The working electrode was a purchased BAS holder normally used for carbon paste. The carbon filaments were packed into the holder cavity at a pressure of 10 MPa without the use of any binder, unless otherwise noted. The circular carbon filament electrode had a surface area of 0.08 cm^2. The CV current densities were calculated by dividing the measured current by the area of the electrode outer surface. Voltammograms began sufficiently negative of the ferricyanide potential to allow reduction of the electroactive species in solution to ferrocyanide. Cycling then began with the oxidation half cycle at scan rates of 20, 50, 75, 100, 125, 150, 175 and 200 mV/s.

Filament packing density was assessed by pressing the filaments into a stainless steel sample cup (0.317 inch in internal diameter and 0.250 inch deep) using a pressure controlled arbor press fitted with a flat tip pressing fixture (0.315 inch in diameter). The pressing pressure was fixed at 10 MPa (the same pressure used to pack the CV working electrode) and the carbon filament weight at 0.05 g. Two displacement transducers (Mitutoyo Digimatics) were used to measure the filament compact thickness under pressure and after pressure release. In the case of the thickness measurement under pressure, the shaft of the pressing fixture tip was affixed to the transducer travel arm using an adaptor to the arm (shown in Fig. 3(a)). The adaptor was configured at a 90° angle and at its end was attached a circular ring into which the pressing fixture shaft was placed. A set screw anchored the pressing fixture shaft to the holding ring. To the second transducer arm was attached a flat circular disk (0.315 inch in diameter) for measuring the filament compact thickness after pressure release (Fig. 3(b)). The empty sample cup was placed, first, under the transducer with the circular disk attached to the arm (Fig. 3(b)) to zero, then under the pressing fixture tip with the affixed transducer arm (Fig. 3(a)) to zero.

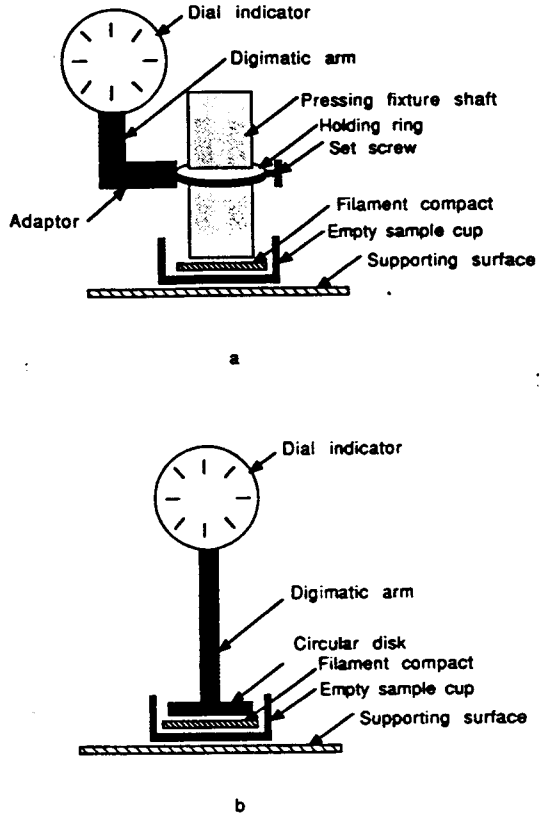

Fig. 3. Set-up for packing density measurement of filament compacts (a) under pressure and (b) after pressure release.

The pressing fixture was raised and the filaments were placed in the sample cup. The pressing fixture was lowered and pressure was applied. The thickness indicated by the transducer was recorded and the pressure released. The sample cup with compacted filaments (now free of pressure) was placed under the transducer arm attached with the circular disk. The arm was lowered to the filament compact surface (no pressure was applied by the transducer arm) and the indicated thickness of the compact was recorded. The amount of spring-back after pressure release was computed by difference, i.e. the thickness after pressure release minus the thickness at pressure. Fractional spring-back was calculated by dividing the computed spring-back by the thickness of the compact at pressure. Packing density was calculated by dividing the weight of the filaments by the volume of the compact.

The rate constant for electron transfer (k_s) was used to evaluate the effectiveness of the cleansing methods. Using the working curve developed by Nicholson and the peak separation values (ΔE) obtained using CV, a corresponding function, Ψ, for each ΔE measured was obtained[39]. According to Nicholson, for the quasi-reversible reaction described in eqn (2),

$$O + ne^- \leftrightarrow R, \qquad (2)$$

eqn (3) can be derived such that

$$\Psi = \gamma^{\alpha} k_s/(\pi a D_O)^{0.5} \quad (3)$$

$$\gamma = (D_O/D_R)^{0.5} \quad (4)$$

where D_O is the diffusion coefficient for the oxidized species, D_R is the diffusion coefficient for the reduced species, a is the coefficient for charge transfer

$$(a = Fv/RT) \quad (5)$$

n is the number of electrons involved in the redox reaction, F is Faraday's constant, v is the CV sweep rate, R = the gas constant and T = the temperature in K.

Using eqn (3), k_s was calculated. Since the difference between the diffusion coefficients for the oxidized and reduced species is generally very small, γ^{α} was considered to be unity. The approximations $D_O = 1.0 \times 10^{-5}$ cm^2/s and F/RT = 39.2 V^{-1} were also used. The scan rate evaluated was 0.2 V/s, and for the redox couple used, $n = 1$.

The capacitance (C) was calculated from the cyclic voltammetry data[37]. C is given by the equation

$$C = dQ/dE \quad (6)$$

where dQ/dE is the rate of change of the surface density of the double layer with electrode potential.

In CV, the electrode potential is varied linearly according to

$$v = dE/dt \quad (7)$$

where v is the potential scan rate. When the scan rate is equal to the rate of change of potential across the double layer, eqns (6) and (7) combine to yield

$$C = (1/v)(dQ/dt) \quad (8)$$

The capacitance current density, i, is equal to dQ/dt; therefore, C is determined by the expression

$$C = i/v \quad (9)$$

C is obtained by measuring i at potentials where no Faradaic reactions occur (in this study, using carbon filaments, at −400 mV using the geometric area to compute current density).

The electrochemical area of the carbon electrode was also calculated from the CV data[40]. CV was conducted under static conditions with a small electrode size in comparison to the electrochemical cell dimensions. Under these conditions, mass transport to the electrode surface (driven by concentration differences) was diffusion controlled and subject to semi-infinite linear diffusion theory. Approximate linear diffusion conditions (conditions with short periods of electrolysis resulting in $it^{\frac{1}{2}}$ constancy) were obtained at −400 mV ± 20 mV, making relative electrochemical area comparisons of the electrode materials and treatment effects possible using the equation

$$A = (it^{\frac{1}{2}})(p^{\frac{1}{2}})/nFD_o^{\frac{1}{2}} C^b \quad (10)$$

where i is the instantaneous current in amperes at −400 mV, t is the time in seconds, n is the number of electrons involved, F is Faraday's constant (96487 coulombs), D_o is the diffusion coefficient (1.0×10^{-5} cm^2/s), C^b is the bulk concentration in mol/mm.

3. RESULTS

3.1 *As-received filaments*

Two types of carbon filament obtained from Applied Sciences Inc. (Cedarville, Ohio) were studied, namely H79 and ADNH. Visually, the ADNH filaments were coherent, resembling cotton wool and were difficult to separate into workable portions of fine clusters. The H79 filaments, on the other hand, were received in the form of clusters and broke into finer agglomerates easily. The TEM images in Fig. 4(a) and 4(b) show the ADNH filaments to be relatively straight and substantially larger in diameter (~1500 Å) and the H79 filaments to be more curved or twisted and smaller in diameter (~500 Å). X-ray diffraction determined the H79 filaments to be more crystalline. Compare the intensity of the 002 graphite peak of ADNH (Fig. 5) with that of H79 (Fig. 6). The small diameter and relatively high degree of crystallinity of the H79 filaments most likely facilitated their breaking into fine agglomerates.

The as-received ADNH, being the less graphitic filament, measured a resistivity (at 7 MPa, Table 1), less than half that of the more graphitic, as-received H79 filament. Typically, a high degree of crystallinity enhances material conductivity, so the results obtained were not expected. Since the smaller diameter H79 filaments have more filament-to-filament contact points than the ADNH filaments, the higher electrical resistance for the H79 filament compact is attributed to the filament-to-filament contact resistance.

The importance of the filament-to-filament contact resistance to the compact's resistivity is better understood when the compact's resistivity is examined as a function of pressure. As shown in Fig. 7, low pressures, up to around 2 MPa, resulted in large disparities between the resistivities of the ADNH and H79 filaments, while pressures beyond 2 MPa generated results with much smaller differences. The filament-to-filament contact resistivity is therefore shown to be more important than volume resistivity in contributing to the compact's resistivity at the low pressures. At the high pressures, on the other hand, volume resistivity becomes more and more important relative to contact resistivity, making the difference in measured values lower.

3.2 *Cleansing of the filaments*

Because filament character affected packing into the working electrode holder, the samples were chopped in deionized water using a rotary blade blender to produce smaller filament lengths and to enhance homogeneous distribution. Both types of filaments felt sticky after the wet processing (the H79 filaments more so than the ADNH filaments), suggesting the presence of a contaminant and the need

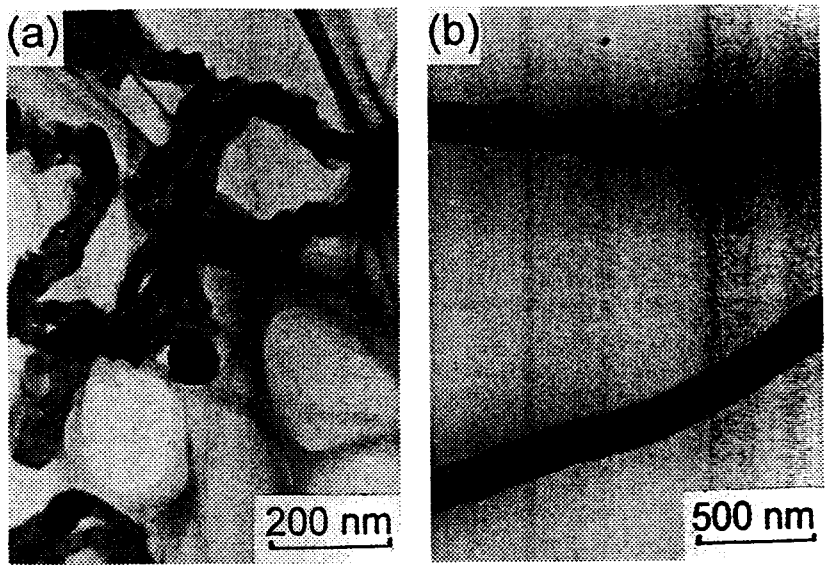

Fig. 4. Transmission electron microscope image of (a) H79 and (b) ADNH filaments.

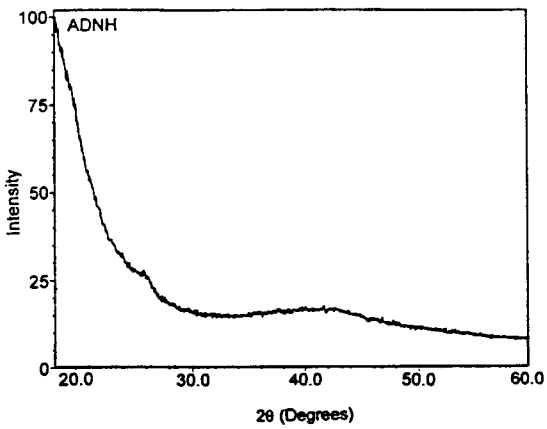

Fig. 5. X-ray diffraction pattern for as-received ADNH.

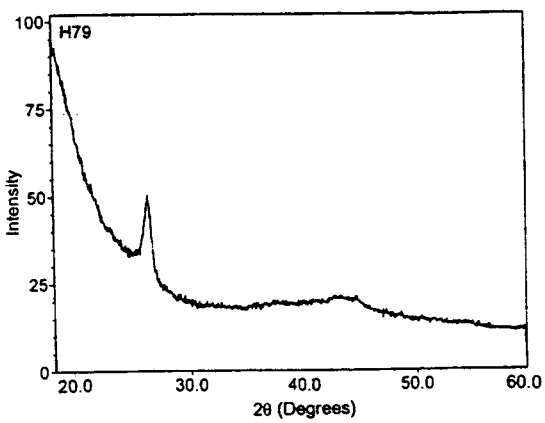

Fig. 6. X-ray diffraction pattern for as-received H79.

for cleansing. SEM examination of the filament surfaces confirmed the presence of the contaminant, with the appearance being similar for both H79 and ADNH. As suspected by Applied Sciences, the contamination was greater for H79. Figure 8 shows the contaminant on H79. The contaminant was randomly spread throughout the filament sample in patches typically larger than the filament diameter and stretching across the width of the filament surface. In addition to being in the patch form, the contaminant was in coating form on the filaments, though the coating form could not be discerned microscopically. It was the coating form that comprised the vast majority of the contaminant. The presence of a contaminant, therefore, was added to the size and crystallinity of the filament as a factor influencing the as-received electrical resistivity measurements.

Acetone was first used to cleanse both ADNH and H79 filaments, but effectiveness in removing the contaminant differed. Whereas acetone proved adequate for the ADNH sample, achieving about a 50% drop in the electrical resistivity after cleansing (Table 1), essentially no difference in the resistivity of the H79 filaments was observed. Cleansing of the filaments in methylene chloride instead of acetone proved more successful for H79, lowering the resistivity by approximately 20% (methylene chloride is a stronger and less polar solvent than acetone). In the case of the ADNH filaments, cleansing in methylene chloride was less effective in decreasing the electrical resistivity than cleansing in acetone (a decrease of 30% using methylene chloride instead of the 50% achieved using acetone). The fractional decrease in the electrical resistivity of ADNH using methylene chloride, however, was still higher than that achieved by cleansing H79 with methylene chloride. Since both samples measured lower resistivities after cleansing, it is clear that the contaminant is another factor influencing the filament electrical resistivity. Cleanliness is not the only factor that affects the resistivity, however, since cleansing with the stronger solvent (methylene chloride) did not result in a lower resistivity for the H79 filaments compared to the ADNH filaments, or a lower resistivity of ADNH compared to acetone cleansed ADNH (Table 1).

Table 1. Electrical resistivity of carbon filaments at 7 MPa pressure

Filament type	Treatment	Density (g/cm^3)	Resistivity (Ω-cm)
ADNH	As-received	0.562	0.041
	Acetone cleansed	0.632	0.020
	Methylene chloride cleansed	0.696	0.029
	Graphitized	0.904	0.0042
H79	As-received	0.795	0.106
	Acetone cleansed	0.733	0.109
	Methylene chloride cleansed	0.889	0.086

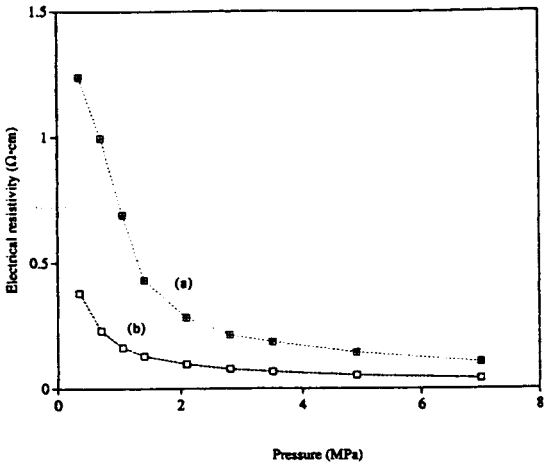

Fig. 7. Electrical resistivity results comparing (a) as-received H79 with (b) as-received ADNH filaments.

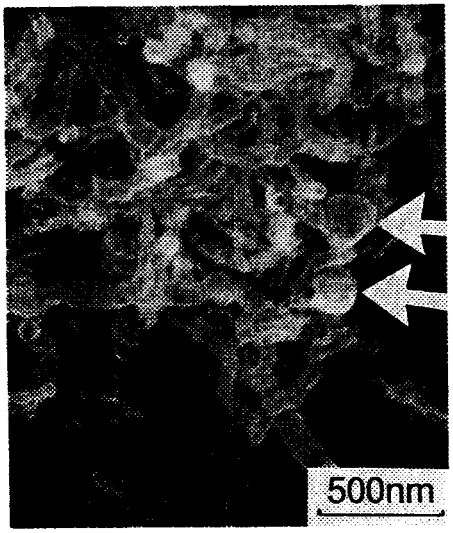

Fig. 8. Scanning electron microscope image of H79 filaments showing contamination.

Solvent cleansing of the filaments not only decreased the filament compact's resistivity, but also removed the stickiness of the wet filaments and darkened the solvent. All three observations indicated that acetone was effective for cleansing ADNH but not H79, whereas methylene chloride was effective for cleansing both ADNH and H79.

The graph in Fig. 9 more clearly shows the effects of cleansing on the electrical resistivity of the H79

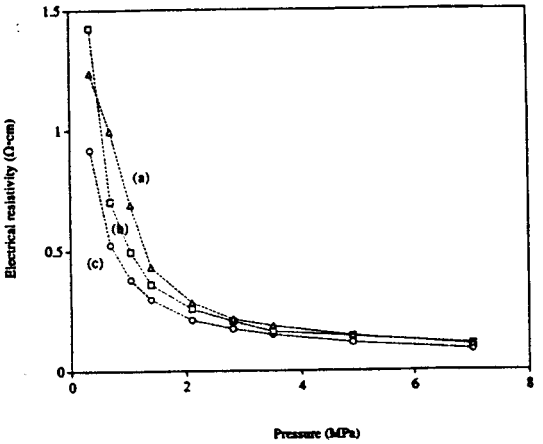

Fig. 9. Electrical resistivity results comparing the effects of cleansing on H79 filaments; (a) as-received, (b) acetone cleansing, (c) methylene chloride cleansing.

filament compact. After using acetone, a slight reduction in the compact's resistivity was observed at low pressures (up to 2 MPa), with no effect at high pressures (beyond the 2 MPa). As with filament size, these results point to the importance of the filament-to-filament contact resistivity contributing to the compact's resistivity of the H79 filaments. Methylene chloride cleansing, on the other hand, yielded even lower resistivity of the H79 compact at all pressures. In the case of ADNH (Fig. 10), acetone cleansing was highly effective in lowering the compact's resistiv-

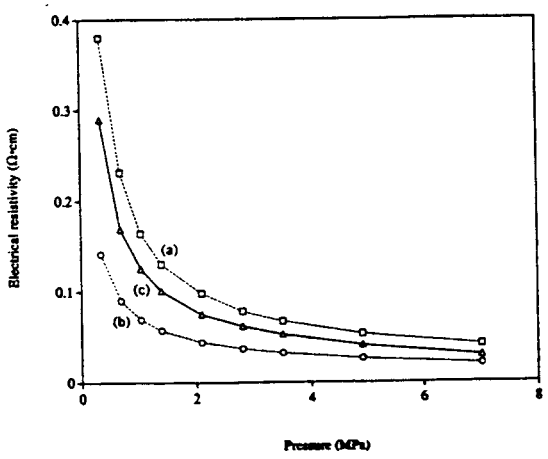

Fig. 10. Electrical resistivity results comparing the effects of cleansing on ADNH filaments; (a) as-received, (b) acetone cleansing, (c) methylene chloride cleansing.

ity, in contrast to H79 (Fig. 9). The effectiveness of cleansing ADNH with acetone was even greater than that of cleansing H79 with methylene chloride (at the low pressures, <2 MPa, 65% decrease in electrical resistivity for acetone cleansed ADNH versus 25% for methylene chloride cleansed H79). The percentage decrease in electrical resistivity (compared to their respective as-received samples) of methylene chloride cleansed ADNH, however, was equivalent to that achieved for methylene chloride cleansed H79, though methylene chloride cleansing of ADNH resulted in an electrical resistivity 70% less than methylene chloride cleansed H79. The fact that acetone cleansing of ADNH resulted in a substantial decrease in resistivity at low pressures (<2 MPa), as well as a marked decrease in resistivity at high pressures (>2 MPa), suggests that ADNH had either a smaller amount of contamination or contamination of a different kind in comparison to H79. The fact that methylene chloride cleansing of ADNH resulted in a lower electrical resistivity compared to the as-received ADNH, but a higher electrical resistivity compared to the acetone cleansed ADNH, suggests that the solvents either result in different surface functional groups or different adsorbed species on the filament surface after cleansing.

FTIR was conducted on the filtrates from the first acetone wash of ADNH and from the first methylene chloride wash of H79. The functional groups identified as dissolved by the respective solvents were essentially the same. Both samples produced spectra for an oxygen-containing organic. FTIR identified the C=O and C−H groups in the contaminant structure. In addition, the ADNH sample was found to contain the C≡N group. (The presence of the C≡N group is consistent with the fact that ADNH is produced from a methane feedstock that also contains some ammonia gas.) The H79 filaments, therefore, were thought to be contaminated with the same basic substance as the ADNH filaments, but the H79 contaminant was apparently composed of a larger molecular unit structure requiring a stronger solvent for removal. GC/MS provided further insight into the contaminant (Table 2 displays the identifications thus made). The major compounds were found to be polyaromatic hydrocarbons with minor components comprising long chain hydrocarbons. Although compositional similarities existed between the two samples, small differences were noted. Present in H79 but absent in ADNH were acenaphthalene with a molecular weight of 152 g/mol and an aliphatic hydrocarbon with a molecular weight of 220 g/mol. The ADNH filaments contained two phthalates (molecular weight = 278 g/mol), identified as diesters of benzene carboxylic acid, while the H79 filaments contained a single phthalate, also a diester of benzene carboxylic acid. These phthalates are believed to be artifacts of the plastic storage container. ADNH was also found to contain, in very minute amounts (and therefore no attempt to identify the compound was made), a nitrogen-containing compound not found in H79. Solvent effectiveness was assessed by comparing the spectra for the contaminant extracted via acetone with that extracted via methylene chloride. The chromatograms for ADNH were identical regardless of the solvent used, whereas those for H79 differed. The acetone extraction was unsuccessful in removing acenaphthene and an aromatic hydrocarbon with a molecular weight of 220 g/mol. Both of these compounds were found in the methylene chloride extract. The results support the idea that the contaminant in the H79 sample requires a stronger solvent for cleansing and that acetone is adequate for the cleansing of ADNH. Cleansing medium effectiveness is also reflected by the electrical resistivity results.

The contaminants found with the Applied Sciences filaments were compared with a tarry substance that accumulated on the reactor inner wall during the filament growth process conducted at the State University of New York at Buffalo (SUNY/Buffalo). The sample contained polyaromatic hydrocarbons, most of which were naphthalene and fluorene. Table 3 summarizes the findings. The differences between this substance and that found with the Applied Sciences filaments may be attributed to differences in the

Table 2. Molecular identifications of contaminants on carbon filaments

Molecular weight (amu)	Identification	Chemical formula	Filament type	
			ADNH	H79
152	Acenaphthalene (aromatic)	$C_{12}H_8$	Absent	Present
220	Aliphatic hydrocarbon		Absent	Present
212	Pentadecane (aliphatic hydrocarbon)	$C_{15}H_{32}$	Present	Present
226	Tetradecane	$C_{14}H_{30}$	Present	Present
240	Aliphatic hydrocarbon		Present	Present
178	Methyl fluorene or phenanthrene	$C_{14}H_{10}$	Present	Present
278	Benzene dicarboxylic acid,	$C_8H_5O_4$	Present	—
	Bis (2-methoxy-ethyl) ester[a]	$C_{14}H_{18}O_2$	Present	Present
202	Fluoranthene (aromatic)	$C_{16}H_{10}$	Present	Present
202	Isomer of fluoranthene	$C_{16}H_{10}$	Present	Present
128	Naphthalene (aliphatic hydrocarbon)	$C_{10}H_8$	Present	Present
180	Fluorenone	$C_{13}H_8O$	Present	Present

[a]Artifacts of plastic storage container.

Table 3. Molecular identifications for tarry residue produced by filament growth process

Molecular weight (amu)	Identification	Chemical formula
116	Aromatic	C_9H_{10}
128	Naphthalene	$C_{10}H_8$
142	Methyl naphthalene	$C_{11}H_{10}$
142	Isomer of methyl naphthalene	$C_{11}H_{10}$
154	Biphenyl or acenaphthene	$C_{12}H_{10}$
152	Acenaphthalene	$C_{12}H_8$
166	Fluorene	$C_{13}H_{10}$
178	Methyl fluorene or phenanthrene	$C_{14}H_{10}$
202	Fluoranthene	$C_{16}H_{10}$

filament growth processing temperature. Further, the SUNY/Buffalo tarry residue sample was collected from the inside of a quartz tube located at the lower temperature end of the processing furnace (temperature is estimated to be between 100 and 200°C). Regardless of the processing parameters, however, it is apparent that the filament growth process generates a residue, composed primarily of polyaromatic hydrocarbons, which influences the electrical properties and could, in turn, produce unfavorable electrochemical results. Acetone was ineffective in totally removing the tarry substance present on glass (as shown visually by noting the darkness of the glass), whereas methylene chloride successfully removed all of the tarry substance. This observation supports the notion of filament cleansing using these solvents, and the notion that methylene chloride was a stronger solvent than acetone.

ESCA results comparing the as-received ADNH filament surface character to that after solvent cleansing (before and after sputter etching to a depth of 20 Å to remove the adventitious carbon) are summarized in Table 4. The data indicate that oxygen was present on the as-received carbon filaments. Since a tarry residue (primarily comprising polyaromatic hydrocarbons) has been identified on the filament surface, the oxygen must then be associated with the tarry residue. Removal of the tarry residue by cleansing caused the atomic oxygen content (after 20 Å removal) to increase from 1.4% as-received to 2.2 and 2.0% after cleansing with acetone and methylene chloride, respectively. This means that removal of the tarry coating by cleansing exposed the oxygen-containing functional groups on the surface of the filaments. The oxygen-containing functional groups enhanced the electrochemical performance, as previously shown for carbon fibers[33].

Given that hydrogen sulfide gas was included with the source gas for growing filaments, the atomic sulfur percentage was also determined by ESCA. The data indicated that acetone cleansing was more effective in removing sulfur residue from the filament surface. As shown in Table 4, the atomic sulfur content before 20 Å removal is 0.1% and after 20 Å removal is 0.0% for acetone cleansed ADNH compared to 0.5% before and 0.4% after for the as-received, and 0.3% both before and after cleansing in methylene chloride. In the case of methylene chloride cleansing, ESCA demonstrated that, before sputter etching, the atomic chlorine content was 0.7%, whereas after 20 Å removal, the atomic chlorine percentage was 0.0%. (Chlorine was not detected by ESCA for either the as-received or acetone cleansed ADNH samples.) The difference in electrical resistivity (reported in Table 1) then may be due to the fact that methylene chloride cleansed ADNH retains some amount of both chlorine and sulfur on the filament surface after cleansing (as opposed to their absence on the filament surface after acetone cleansing).

3.3 *Structure of the filaments*

The crystallographic structure of the ADNH filaments after graphitization was assessed by x-ray diffraction and compared with its as-received version and with the as-received H79. The x-ray diffraction pattern for the graphitized ADNH (Fig. 11) shows the 002 graphite peak to be substantially higher in intensity than the as-received ADNH (Fig. 5), indicat-

Table 4. Surface oxygen, sulfur and chlorine concentration for ADNH filaments as assessed by ESCA before and after removal of the top 20 Å

	Oxygen[a] (at.% ± 0.1)		Sulfur (at.% ± 0.1)		Chlorine (at.% ± 0.1)	
Treatment	Before removal	After removal	Before removal	After removal	Before removal	After removal
As-received	1.9	1.4	0.5	0.4	0.0	0.0
Acetone cleansed	2.8	2.2	0.1	0.0	0.0	0.0
Methylene chloride cleansed	2.8	2.0	0.3	0.3	0.7	0.0

[a]Using the O1*s* peak at 533.5–534.5 eV. Adsorbed oxygen corresponds to the O1*s* peak observed at 532.4–533.3 eV; it was not totally removed because of the valleys between adjacent units in the compact.

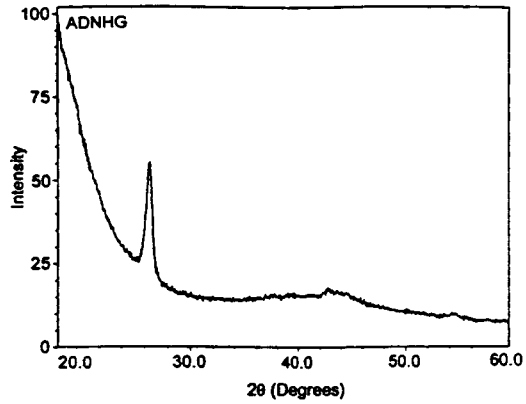

Fig. 11. X-ray diffraction pattern for graphitized ADNH filaments.

ing a marked increase in crystallinity after graphitization. Although the degree of crystallinity of ADNH is increased after graphitization, TEM results show that the preferred orientation of the planes remained unchanged. The electrical resistivity of the graphitized ADNH (Table 1) was lower than the acetone washed ADNH, demonstrating that the degree of crystallinity influences the electrical character.

The peak intensity of the graphitized ADNH (Fig. 11) as compared to the as-received H79 (Fig. 6) is slightly higher and the peak width is smaller, indicating, respectively, a higher crystallinity and a larger grain size for the graphitized ADNH than the as-received H79. The electrical resistivity of the graphitized ADNH was much lower than the methylene chloride washed H79 (Fig. 12 and Table 1). These results indicate that even though the level of crystallinity has an influence on electrical resistivity (graphitized ADNH generating lower resistivity values than cleansed, ungraphitized ADNH), filament diameter is also an important factor (graphitized ADNH of 1500 Å diameter yielding much lower resistivity results than cleansed, crystalline H79 filaments of 500 Å diameter). Review of all the electrical resistivity

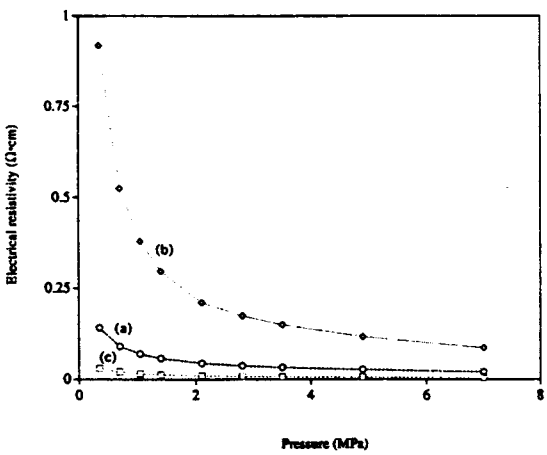

Fig. 12. Electrical resistivity results comparing (a) acetone washed ADNH filaments, (b) methylene chloride washed H79 filaments, and (c) graphitized ADNH filaments.

results shows that the consistently higher electrical resistivities of the H79 filament compacts are primarily attributed to their small diameter, with additional influence made by the presence of a contaminant, and only some influence made by the level of crystallinity.

3.4 *Cyclic voltammetry and filament compactability*

Packing the as-received ADNH filaments into the electrode holder proved more difficult than packing the as-received H79 filaments. The clinginess of the ADNH and its resistance to fracture imparted a resistance to compaction that was not observed with the H79 filaments. After compaction at 10 MPa and upon pressure release, the ADNH compact partially sprang back, causing a part of the compact to protrude out of the electrode cavity. (The protruded portion was removed before cyclic voltammetry.) Acetone and methylene chloride cleansing decreased the fractional spring-back (methylene chloride having twice the effect of acetone), and also increased the packing density both at pressure and after pressure release, relative to the corresponding value before cleansing (Table 5). The poor CV result of the as-received ADNH (Table 6 and Fig. 13(a)) is partly due to the low packing density (Table 5). Note that the densities reported in Table 5 differ from those in Table 1. The higher at-pressure density values of Table 5 compared to Table 1 are attributed to the higher pressure (10 MPa) in Table 5.

In Fig. 13(a), the curve with the lowest positive peak current density is associated with the 20 mV/s scan, whereas the highest positive peak current density is associated with the 200 mV/s scan. A high residual current is associated with an essentially irreversible electrochemical response ($\Delta E_{200\ mV/s}$ = 530 mV and I_a/I_c = 4.7, Table 6). The poor packing density was most likely the primary contributor to the high residual current and only a partial contributor (contamination and a lower level of crystallinity also playing a role) to the lack of reversibility.

The packing density of H79 showed very little change after pressure release (Table 5), and electrochemically the H79 type filaments (Fig. 13(b)) demonstrated better reversibility than did the ADNH filaments (Fig. 13(a); $\Delta E_{200\ mV/s}$ = 110 mV and I_a/I_c = 1.4, Table 6). As indicated by the packing density study, and confirmed using CV, compactability was not a problem. As mentioned earlier, their smaller diameter and higher degree of crystallinity most likely facilitated their breaking into finer agglomerates. This coupled with their inherently curved and twisted shape (providing good filament-to-filament connectivity) helped packing of the electrode cavity and density retention after pressure release.

Figure 14(a) and (b) displays both filament types after acetone cleansing. Note that after cleansing the extraneous current density at the negative potential of the H79 sample is eliminated (Fig. 14(b)); however, the reaction becomes less reversible ($\Delta E_{200\ mV/s}$ = 190,

Table 5. Packing density of as-received and treated filaments compacted at 10 MPa[a]

Filament type and treatment	Packing density (g/cm³) (±0.002) Under pressure	After pressure release	Fractional spring-back upon pressure release (±0.002)
ADNH			
As-received	0.581	0.465	0.249
Acetone cleansed	0.743	0.680	0.092
Acetone cleansed and then chopped	0.747	0.737	0.014
Methylene chloride cleansed and then chopped	0.825	0.820	0.006
Graphitized	1.112	1.104[b]	0.007
H79			
As-received	0.973	0.972	0.001
Acetone cleansed	0.882	0.878	0.004
Methylene chloride cleansed	1.129	1.128	0.001

[a]A high packing density corresponds to good compactability.
[b]No compact integrity was present; upon release of pressure, loose filaments covered the surface of the compact and the compact could not be handled.

Table 6. Carbon filament cyclic voltammetry results obtained at a potential scan rate of 200 mV/s

Filament type and treatment	Anodic peak current density I_a (mA/cm²) (±25)	Cathodic peak current density I_c (mA/cm²) (±25)	I_a/I_c (±0.2)	Peak separation ΔE (mV) (±10)
ADNH				
As-received	7800	1650	4.7	530
Acetone cleansed	13580	8470	1.6	200
Acetone cleansed and then chopped	1680	1450	1.2	130
Methylene chloride cleansed and then chopped	2000	1750	1.1	90
Graphitized (with binder)	490	300	1.6	600
H79				
As-received	2930	2040[a]	1.4	110
Acetone cleansed	960	730	1.3	190
Methylene chloride cleansed	1680	1290	1.3	150

[a]With high residual current density up to 7700 mA/cm² at potentials below −0.4V.

Table 6) and more dependent on scan rate. In addition, ΔE consistently increases with increasing scan rate, and the material now carries a lower current density. The CV results coupled with the results from FTIR and GC/MS indicate that acetone cleansing incompletely removed the tarry substance coating the H79 filaments. This resulted in the largest degree of spring-back for the H79 filaments (Table 5). Incomplete cleansing of the residue is shown to negatively impact on reaction reversibility and electrode kinetics, even though the high onset current at low potentials (Fig. 13(b)) is eliminated.

To further improve the electrochemical response of H79, methylene chloride, a stronger and less polar solvent, was used to cleanse the filaments. The result was the successful removal of the tarry substance coating the H79 filaments, as evidenced by the decreased compact electrical resistivity (Table 1), the increased packing density after cleansing (Table 5), the elimination of the extraneous current density observed in the as-received sample, the restoration of the reaction reversibility and a portion of the current density capability (Table 6), and the elimination of the scan rate dependence observed after acetone cleansing (Fig. 15(b)).

To summarize, then, of the three conditions evaluated for the packing capability of H79 (Table 5), the largest degree of spring-back was observed for the acetone cleansed sample. The as-received H79 filaments displayed a high current density at the start of CV testing at highly negative potentials (Fig. 13(b)) even though reversibility (Table 6) and kinetics (k_s = 0.0125 cm/s, Table 7) were good. This current is attributed to the electrochemical oxidation of the contaminant present. An attempt to completely remove the contaminant from the H79 filaments using acetone was unsuccessful. The incomplete removal of the contaminant from H79 using acetone resulted in a slightly higher electrical resistivity (Table 1) and a lower packing density (Table 5) than the as-received version. CV shows that even though the high current density at the highly negative potentials have been eliminated by acetone cleansing (Fig. 14(b)), the slightly increased electrical resistivity (Table 1) and the lower packing density (Table 5) resulted in a less reversible reaction (Table 6) and a

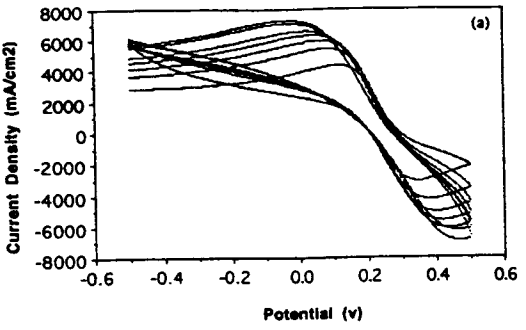

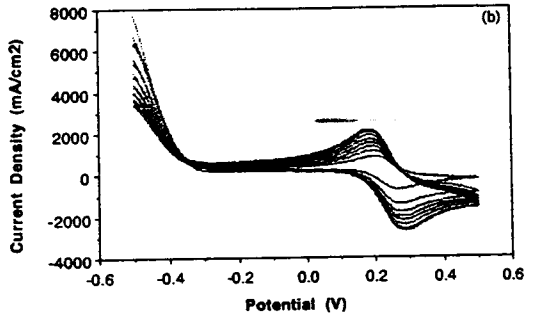

Fig. 13. Cyclic voltammetry results for (a) as-received ADNH filaments and (b) as-received H79 filaments.

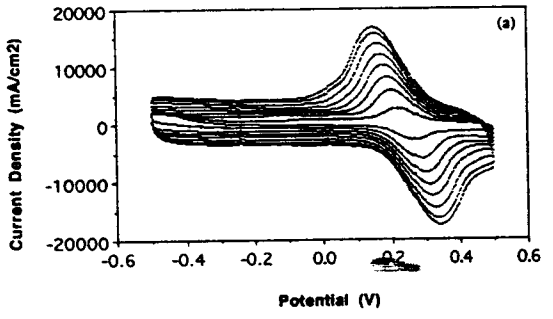

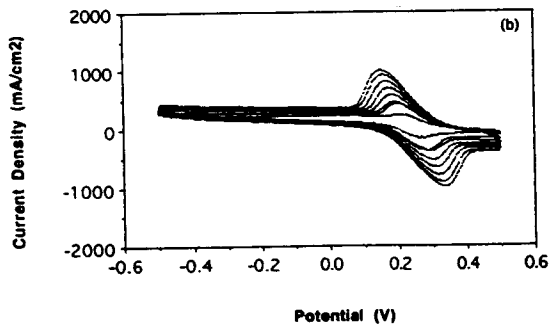

Fig. 14. Cyclic voltammetry results for (a) acetone cleansed ADNH filaments and (b) acetone cleansed H79 filaments.

decrease in the reaction kinetics ($k_s = 0.0043$ cm/s, Table 7) at the acetone cleansed H79 CV electrode. Methylene chloride cleansing successfully removed the contaminant from H79, effectively lowering the

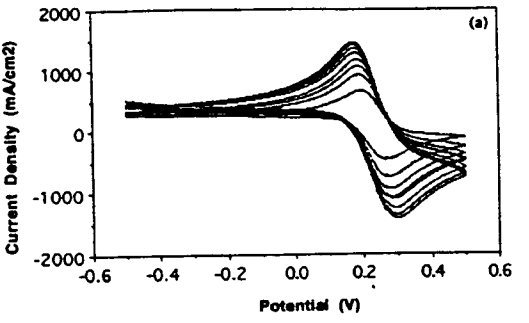

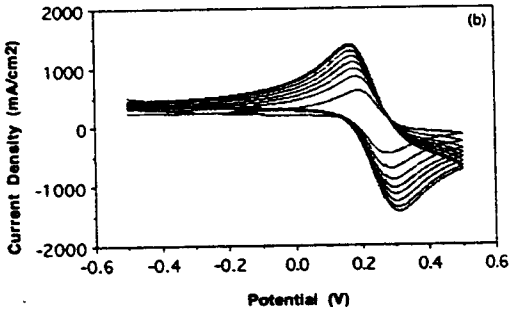

Fig. 15. Cyclic voltammetry results for (a) acetone cleansed and chopped ADNH filaments and (b) methylene chloride cleansed H79 filaments.

electrical resistivity of the compact (Table 1) and producing a denser packing with little fractional spring-back (Table 5). The high current density at the highly negative potentials was also eliminated by methylene chloride cleansing (Fig. 15(b)) and the reversibility (Table 6) and reaction kinetics ($k_s = 0.0065$ cm/s, Table 7) were partially restored; however, reversibility and reaction kinetics were not equivalent to those displayed by the as-received H79, supporting the conclusion that cleansing alone was not sufficient for achieving good electrochemical performance. The electrical resistivity of the compact, which was four times greater for the methylene chloride cleansed H79 than for the acetone cleansed ADNH (Table 1), also influenced electrochemical capability.

In contrast to H79, acetone cleansing of the ADNH filaments resulted in improvement of both the reaction reversibility ($\Delta E_{200\ mV/s} = 200$ mV and $I_a/I_c = 1.6$, Table 6 and Fig. 14(a)) and the electrode packing density (0.680 g/cm^3 as opposed to the as-received 0.465 g/cm^3, Table 5). The increased packing density is consistent with the fact that the wet filaments became less sticky after cleansing. Even though the tarry residue was removed from the filament surface (improving electrode kinetics) and more filaments were able to fit into the electrode cavity (improving packing density), the results were insufficient to substantially diminish the residual current density. The large filament agglomerates (in comparison to those characteristic of H79 filaments)

Table 7. Electrochemical behavior of carbon filaments

Filament type and treatment	k_s (cm/s) ±0.0002	Capacitance[a] (μF/cm^2) ±0.05	Electrochemical area[b] (cm^2) ±5
ADNH			
As-received	Irreversible	5.93	65
Acetone cleansed	0.0037	27.30	298
Acetone cleansed and then chopped	0.0082	1.92	30
Methylene chloride cleansed and then chopped	0.0209	2.62	29
Graphitized	Irreversible	1.39	152
H79			
As-received	0.0125	2.41	38
Acetone cleansed	0.0043	1.36	21
Methylene chloride cleansed	0.0065	1.96	31

[a]Calculated using geometric area.
[b]Geometric area = 0.0792 cm^2.

continue to negatively influence the electrochemical behavior of ADNH.

To further improve the packing density (and therefore the subsequent CV) of ADNH, the cleansed filaments were placed in a rotary blender filled with acetone and chopped by blending for 3 minutes. The scanning electron microscope (SEM) was used to compare the blended filaments with the as-received filaments. The blended filaments were deemed to be shorter than the as-received version by virtue of the fact that, under the same magnification, the ends of the blended filaments were discernible, whereas those of the as-received version were not. The inability to separate the as-received ADNH filaments precluded measurement of the as-received filament length, so the change in length resulting from the chopping process was not quantifiable. Table 5, however, shows that chopping the cleansed ADNH filaments resulted in an additional increase in packing density after spring-back when compared to the sample subjected only to the acetone cleansing process. This additional increase in packing density is due to the large decrease in fractional spring-back (Table 5). Furthermore, chopping decreased the residual current density (Fig. 15(a) compared to Fig. 14(a)) and increased the reversibility and rate constant k_s (Table 7). The improved electrochemical behavior after chopping is partly due to the increased packing density. Comparing ADNH CV results with those of H79 (Fig. 15(b) compared to Fig. 15(a), see also Tables 6 and 7), it is clear that the acetone cleansing with chopping of ADNH and the methylene chloride cleansing of H79 produced essentially equivalent electrochemical behavior.

The effects of cleansing media on the packing density of ADNH is shown in Table 5. Cleansing and chopping of ADNH in methylene chloride resulted in an increase in packing density by approximately 10% from that obtained using acetone, or an overall increase in packing density of about 30% from the as-received sample. More dramatically, the fractional spring-back of ADNH after cleansing and chopping in methylene chloride decreased by 60% from that of acetone, and 98% from that observed for the as-received ADNH (Table 5). The improvements achieved using methylene chloride to cleanse ADNH is reflected in the CV response as well. As shown by comparing Fig. 15(a) (acetone) with Fig. 16 (methylene chloride), cleansing and chopping of ADNH in methylene chloride resulted in better reversibility (by more than 30%) and less dependence upon scan rate than achieved using acetone; but more importantly, the rate constant of ADNH after methylene chloride cleansing and chopping increased by 460%, from 0.0037 to 0.0209 cm/s (Table 7).

The improvement in electrochemical performance of ADNH realized by cleansing in methylene chloride is significantly greater than that achieved for H79. For H79, the methylene chloride cleansing removed the high residual current density at potentials below −0.4 V, but decreased the rate constant by 50%. The difference between the responses of ADNH and H79 is attributed partly to the difference in their respective filament diameters, and, therefore, their filament-to-filament contact resistivity, and probably partly to the differences in crystallinity. The origin of the difference is not totally clear.

In relating the CV results relative to solvent cleansing to the electrical resistivity and ESCA results, two conclusions are drawn. First, a high packing density of the carbon electrode and a low compact

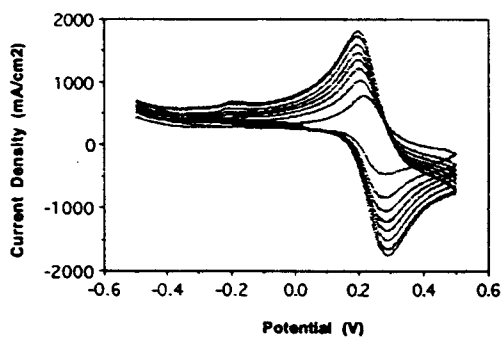

Fig. 16. Cyclic voltammetry results for methylene chloride cleansed ADNH filaments.

resistivity are important to attaining good electrochemical behavior. A smaller filament diameter (H79 compared to ADNH), a smaller filament length (obtained by chopping ADNH) and greater surface cleanliness (obtained by solvent cleansing) enhanced the packing density; a smaller filament diameter increased the compact resistivity, while greater cleanliness decreased the compact resistivity. Second, electrochemical reversibility of the iron cyanide redox couple was enhanced by the filament cleansing process, provided that the compact resistivity was sufficiently low (as for ADNH, as opposed to H79). The enhanced reversibility is due to the removal of a tarry residue native to the filament growth process, provided that the compact resistivity was sufficiently low (as for ADNH, as opposed to H79). The actual carbon filament surface, which has oxygen-containing functional groups, becomes exposed by the cleansing process, thereby enhancing the electrochemical reversibility; although the tarry residue does have associated with it oxygen-containing surface functional groups, their presence is ineffective in improving the electrochemical response.

The graphitization process performed on the ADNH carbon filaments provided additional insight into the factors influencing the electrochemical performance. The first effect of graphitization was the loss of connectivity. The graphitized filaments could not be retained within the electrode cavity without the use of a binder, so paraffin oil was used. As shown by the CV results in Fig. 17 and Tables 6 and 7, graphitization of ADNH, which was expected to enhance the electrochemical performance, actually degraded it. Furthermore, this degradation occurred in spite of an increased packing density (Table 5) and a decreased compact resistivity (Table 1). Therefore, the possible effect of graphitization on the surface chemistry was considered, although graphitization must be accompanied by decomposition and carbonization of the tarry residue. To validate this possibility, oxidation of the graphitized filaments was conducted by heating in air at 450°C for 1 hour. (It is known that oxygen-containing surface functional groups on carbon surfaces enhance electrochemical performance.) Indeed partial restoration of the electrochemical capability occurred after the oxidation heat-treatment (Fig. 18). A binder was still required to hold the filaments within the electrode cavity.

The results obtained with the ADNH filaments after graphitization relate to those obtained using H79 filaments. First, the ease with which the ADNH filaments broke into smaller lengths after graphitization supports the earlier conclusion drawn for H79, i.e. that the higher level of crystallinity of the H79 filaments facilitated their breakage. Second, the physical character of the filaments plays a role in packing density and compaction integrity. The smaller diameter and the curved and twisted shape of the H79 filaments interacted to allow efficient packing density and retention of a good compact within the electrode holder cavity without the use of a binder, even though the H79 filaments have a higher level of crystallinity. The smaller degree of filament twisting and curving in conjunction with the larger diameter of the ADNH filaments interacted to negatively impact on packing density and compaction integrity. Increased crystallinity and grain size further degraded compact integrity. Success in compaction was achieved by chopping the ADNH filaments into shorter lengths.

The effectiveness of the cleansing methods was assessed by computing changes in the rate constant for electron transfer, k_s, across the filament electrode surface. As Nicholson relates, the value of k_s decreases as ΔE increases and ΔE increases, and as electron transfer rate decreases. Consequently, effectiveness is indicated by higher k_s values. Results are included in Table 7. Note that acetone cleansing of ADNH improved electrode kinetics ($k_s = 0.0037$ cm/s after acetone cleansing versus the response being irreversible as-received). Reaction kinetics for the H79 electrode, however, were negatively impacted by cleansing. Further supporting these results are the electrochemical areas (A) computed from the CV data. In the case of acetone cleansing of ADNH, the electrochemical area of the electrode increased from 65 to 298 cm^2 (Table 7), but decreased in the case of H79 from 38 to 21 cm^2. This difference between ADNH and H79 is consistent with the effectiveness of acetone cleansing to ADNH and the ineffectiveness

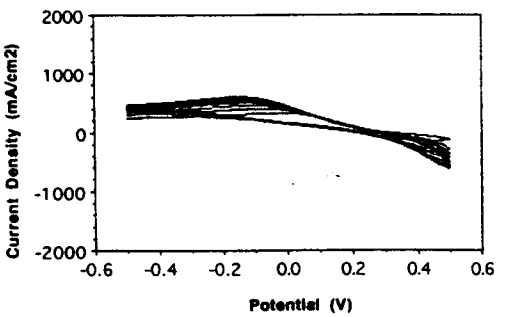

Fig. 17. Cyclic voltammetry results for graphitized ADNH filaments.

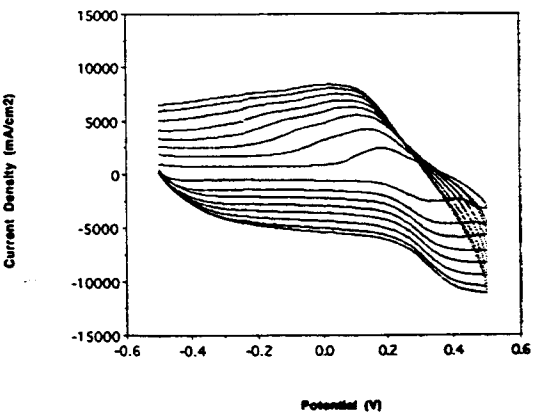

Fig. 18. Cyclic voltammetry results for graphitized and subsequently oxidized ADNH filaments.

of acetone cleansing to H79. The large value of A for acetone cleansed ADNH is probably related to the improved wetting by the electrolyte after the cleansing. Improved wetting is also suggested by the increase in surface oxygen concentration (Table 4). On the other hand, chopping of the acetone cleansed ADNH greatly decreased A, while increasing k_s; both effects are attributed to the increase in packing density after pressure release (Table 5). The only advantage that cleansing had on the H79 filament electrochemical response was the removal of the high current densities at the highly negative voltages. Comparison of the cleansing media demonstrates methylene chloride to be more effective than acetone, with a more dramatic effectiveness observed for ADNH where the rate constant increased to 0.0209 cm/s using methylene chloride for cleansing. Methylene chloride cleansing significantly improved kinetics in the ADNH case, while the electrochemical area was decreased. The low value of A for methylene chloride cleansed ADNH is probably due to the presence of chlorine (Table 4), which affected the wetting by the electrolyte. Graphitization of ADNH increased A but rendered the response irreversible; the former effect is attributed to the increased crystallinity and the consequent exposure of basal plane edges, which are more electrochemically active than the basal plane itself; the latter effect is attributed to the change in surface functional groups.

A high electrochemical area tends to be correlated with a high capacitance, though there are exceptions, such as graphitized ADNH (Table 7). In particular, a significant increase in the capacitance of ADNH after acetone cleansing (without chopping) was observed. This is reasonable since high capacitance is associated with high concentration of oxygen-containing surface functional groups[37], and acetone cleansing increased this oxygen concentration (Table 4).

The carbon filament electrode kinetics after cleansing and/or chopping are comparable to, and in the case of methylene chloride cleansing and chopping of ADNH, significantly better than those obtained with other carbon materials. Previous studies using rotated disk carbon paste electrodes, for example, demonstrate k_s for ferri-ferrocyanide in 0.1 M KCl to be about 0.0015 cm/s[40]. For a stationary carbon paste electrode tested in a 0.5 mM solution of ferrocyanide in 0.1 M KCl at scan rates between 4.5 and 45 mV/s, the k_s values ranged from 0.0016 cm/s (22.5 mV/s) to 0.0024 cm/s (45 mV/s)[41]. The rate constant for ferricyanide reduction on glassy carbon in a 0.5 M K_2SO_4 electrolyte was 0.0025 cm/s[42]. In the case of ADNH, acetone cleansing and chopping decreased the electrochemical area of the electrode, which again is expected given the increase in packing density (Table 5).

4. DISCUSSION

In contrast to the speculation of Applied Sciences Inc.[21], the contamination on the carbon filaments was not soot, but a tarry material (mostly polyaromatic hydrocarbons, as shown by mass spectrometry and supported by FTIR). Soot cannot be dissolved by acetone or methylene chloride. Solvent cleansing was found to be a simple and effective method of surface treatment for the purpose of removal of the tarry coating left behind by the carbon filament growth process involving carbonaceous gases. That the filament growth process is responsible for the tarry coating was shown by the presence of a similar tarry substance on the inner wall of the filament growth chamber. That solvent cleansing was indeed a removal process rather than a surface modification process was indicated by: (1) the black tarry substance that was present in the (originally colorless) solvent after cleansing, (2) visual observation that a glass surface covered with the tarry substance became colorless again after cleansing, (3) the wet filaments becoming less sticky after cleansing, and (4) GC/MS analysis of the solvent after cleansing. The cleansing served to decrease the filament compact's electrical resistivity, expose the oxygen-containing functional groups on the surface of the carbon filaments, enhance the filament compactability, and, in the case of ADNH, decrease the fractional spring-back of the compact upon pressure release. Such a cleansing treatment is also applicable to other carbons, such as vitreous carbon made from polymeric foam (Energy Research and Generation, Inc., Oakland, California), as described in a companion paper[42]. (For conventional carbon fibers made from pitch, namely Amoco's Thornel P-100, the cleansing treatment had no effect, indicating the absence of a tarry residue.)

The solvent for cleansing should be one that is capable of dissolving polyaromatic hydrocarbons. They can be acetone, methylene chloride, toluene, etc. Methylene chloride is a better solvent (less polar) then acetone, so it is more capable of removing tenacious tarry coatings. The tenacity of the coating is believed to be greater when the polyaromatic hydrocarbons are larger in molecular weight. The tenacity varies among different grades of carbon filaments made from carbonaceous gases. In the case of carbon filaments made by Applied Sciences Inc., H79 has a more tenacious coating than ADNH, and so requires methylene chloride for cleansing, whereas acetone suffices for ADNH. The difference in coating nature between H79 and ADNH is probably related to the difference in surface oxygen and surface nitrogen contents claimed by Applied Sciences Inc.

The tarry coating was found to strongly affect the electrochemical behavior, the electrical resistivity of the filament compact and the compactability of the filaments. Cleansing of ADNH improved the electrochemical reversibility and increased the electron transfer rate; cleansing of H79 decreased the current density at potentials away from the voltammetric peaks. Cleansing also decreased the electrical contact resistivity between adjacent filaments at a given contact pressure and improved filament compactability

at a given compaction pressure. All three effects of cleansing benefit the performance of electrodes made from the filaments.

Graphitization heat treatment at >2500°C is a common method for improving the crystallinity of carbons. In this work, it was found that graphitization degraded the electrochemical performance of carbon filaments, in spite of the decrease of the filament compact's electrical resistivity (mainly decrease of the volume electrical resistivity of the filaments, as the volume resistivity is known generally to decrease with increasing crystallinity and filament compactability). This negative electrochemical effect is attributed to a change in the surface functional groups after the graphitization heat treatment. The change in the surface functional groups also affects the contact resistivity, and hence affects the compact's electrical resistivity.

This work has shown the importance of a low electrical contact resistivity between conducting units in an agglomerate (as varied by cleansing) and a low contact resistance within the entire agglomerate (as varied by varying the filament diameter) in order for the agglomerate to exhibit good electrochemical performance. A low volume electrical resistivity alone is not sufficient. The volume resistivity depends on the bulk properties, such as the crystallinity. On the other hand, the contact resistivity depends on the surface conditions, such as cleanliness and functional groups. A high contact resistivity results in a lower voltammetric peak current density.

The compactability of the filaments is important for the electrochemical performance of the filament compact, since a higher compactability means that a greater number of filaments are exposed per unit area of the electrode's outer surface. A low packing density results in a high residual current density. The compactability of the filaments (both under pressure and after pressure release) was found to be improved by cleansing the filaments (with acetone or methylene chloride in the case of ADNH, and with methylene chloride in the case of H79). Chopping the filaments in a liquid medium (acetone or methylene chloride) in a rotary blender helped decrease the fractional springback of the compact after pressure release, due to the decrease in filament length. However, the chopping step was necessary only if the filaments were relatively straight and large in diameter (i.e. ADNH as opposed to H79).

Commonly used for analytical work are carbon paste electrodes, which are made from graphite particles and require a binder (an oil) for formability and resistance to electrolyte penetration. In contrast, the carbon filament electrodes do not require any binder, except for graphitized ADNH, which exhibits poor electrochemical performance anyway. The absence of a binder is an advantage in work where binders or oils may be incompatible with the medium under study.

Commonly used for analytical work are carbon paste electrodes, which are made from graphite particles and require a binder (an oil) for formability and resistance to electrolyte penetration. In contrast, the carbon filament electrodes do not require any binder, except for graphitized ADNH, which exhibits poor electrochemical performance anyway. The absence of a binder is an advantage in work where binders or oils may be incompatible with the medium under study.

Carbon filaments without cleansing are almost commercially available (currently in pilot plant scale in Applied Sciences Inc.), but the solvent cleansing necessary to improve their electrochemical behavior is an inexpensive process, and so adds to the cost of the filaments. When in full production, the carbon filaments are expected to cost below U.S. $5/lb, according to Applied Sciences Inc.

5. CONCLUSIONS

Vapor-grown carbon filaments were found to be covered with a tarry coating (mostly polyaromatic hydrocarbons), which degraded electrochemical behavior. The tarry coating increased the contact resistivity between adjacent filaments in a filament compact at a given contact pressure. The removal of the tarry coating was achieved by solvent cleansing. The coating removal caused the exposure of oxygen-containing functional groups on the surface of the carbon filaments and improved filament compactability. The tenacity of the tarry coating was greater for the H79 filaments, which required use of a stronger solvent, namely methylene chloride. Acetone cleansing was effective for ADNH filaments, though further improvement was observed by cleansing in methylene chloride. Filament electrochemical performance was greatly enhanced by solvent cleansing, as shown by CV conducted with the iron cyanide redox couple, as a result of the exposure of the oxygen-containing functional groups and improved filament compactability. Chopping the ADNH filaments in a liquid medium using a blender further enhanced filament compactability after pressure release, thereby further improving the electrochemical performance. Chopping was less important for H79 than ADNH. The electrochemical performance improvement encompassed increased reversibility and electron transfer rate (in the case of ADNH) and decreased magnitude of the current density at potentials away from the CV peaks (in the case of H79). For example, acetone cleansing changed the CV response of ADNH from being irreversible to being reversible with a rate constant $k_s = 0.0037$ cm/s. Methylene chloride cleansing further improved the electrochemical response of ADNH by increasing the rate constant, k_s, to 0.0209 cm/s. Graphitization degraded the electrochemical performance, even though it decreased the filament compact's electrical resistivity and increased the compactability, owing to the change in surface functional groups. Finally, carbon filament compacts (if not graphitized) did not require any binder or oil

for good electrochemical performance, in contrast to carbon paste electrodes.

Acknowledgements—The authors would like to thank New York State Energy Research and Development Authority for funding part of this work, and St. Mary's Carbon Co. for graphitization treatment of the carbon filaments.

REFRENCES

1. D. L. Trimm, *Catal. Rev. Sci. Engng* **16**, 155 (1977).
2. R. T. K. Baker and P. S. Harris, *Chem. Phys. Carbon* **14**, 83 (1978).
3. C. H. Bartholomew, *Catal. Rev. Sci. Engng* **24**, 67 (1982).
4. E. F. Wolf and P. Alfani, *Catal. Rev. Sci. Engng* **24**, 329 (1982).
5. R. T. K. Baker, D. J. C. Yates and J. A. Dumesic, *Coke Formation on Metal Surfaces*, American Chemical Society (1982).
6. W. R. Ruston, M. Warzee, J. Hennaut and J. Waty, *Carbon* **7**, 47 (1969).
7. S. D. Robertson, *Carbon* **8**, 365 (1970).
8. R. T. K. Baker, M. A. Barber, F. S. Feates, P. S. Harris and R. J. Waite, *J. Catal.* **26**, 51 (1972).
9. J. R. Rostrup-Nielsen, *J. Catal.* **27**, 343 (1972).
10. R. T. K. Baker, P. S. Harris, R. B. Thomas and R. J. Waite, *J. Catal.* **30**, 86 (1973).
11. C. W. Keep, R. T. K. Baker and J. A. France, *J. Catal.* **47**, 232 (1977).
12. R. T. K. Baker, M. A. Barber, P. S. Harris, F. S. Feates and R. J. Waite, *J. Catal.* **26**, 51 (1972).
13. J. R. Rostrup-Nielsen, *J. Catal.* **27**, 343 (1972).
14. A. Oberlin, M. Endo and T. Koyama, *J. Cryst. Growth* **32**, 335 (1976).
15. S. D. Jackson, S. J. Thompson and G. Webb, *J. Catal.* **70**, 249 (1981).
16. M. Audier and M. Coulon, *Carbon* **23**, 317 (1985).
17. L. S. Lobo and D. L. Trimm, *J. Catal.* **29**, 15 (1973).
18. G. G. Tibbetts, *J. Cryst. Growth* **66**, 632 (1984).
19. G. G. Tibbetts, M. G. DeVour and E. J. Rodda, *Carbon* **25**, 367 (1987).
20. J. R. Bradley and G. G. Tibbetts, *Carbon* **23**, 423 (1985).
21. R. L. Alig, private communication (1995).
22. G. G. Tibbetts, D. W. Gorkiewicz and R. L. Alig, *Carbon* **31**, 809 (1993).
23. M. Endo, J. Nakamura and A. Emori, *Extended Abstracts and Program, 21st Bienniel Conference on Carbon*. American Carbon Society (1993).
24. M. Endo, H. Nakamura, A. Emori, S. Ishida and M. Inagaki, *TANSO* **150**, 319 (1991).
25. X. Shui, D. L. Chung and C. A. Frysz, *J. Power Sources* **47**, 313 (1994).
26. C. S. Hahn, H. S. Cho and H. S. Yang, *Carbon* **19**, 225 (1981).
27. G. Norwitz and M. Galan, *Carbon* **5**, 287 (1967).
28. S. Hagiwara, K. Tsutsumi and H. Takahashi, *Carbon* **16**, 89 (1978).
29. Y. Matsumura, S. Hagiwara and H. Takahashi, *Carbon* **14**, 163 (1976).
30. B. R. Puri and R. C. Bansal, *Carbon* **1**, 457 (1964).
31. G. Kaye, *Carbon* **2**, 413 (1978).
32. K. Kinoshita, *Carbon Electrochemical and Physicochemical Properties*. John Wiley and Sons, New York (1988).
33. C. A. Frysz, X. Shui and D. D. L. Chung, *Carbon* **32**, 1499 (1994).
34. R. L. McCreery, In *Electroanalytical Chemistry* (Edited by A. J. Bard), p. 306. Marcel Dekker, New York (1989).
35. T. G. Strein and A. G. Ewing, *Anal. Chem.* **63**, 194 (1991).
36. R. M. Wightman, M. R. Deakin, P. M. Kovach, W. G. Kuhr and K. J. Stutts, *J. Electrochem. Soc.* **131**, 1578 (1984).
37. K. Kinoshita, *Carbon Electrochemical and Physicochemical Properties*. John Wiley and Sons, New York (1988).
38. W. R. Runyan, *Semiconductor Measurements and Instrumentation*. McGraw-Hill, New York (1976).
39. R. S. Nicholson, *Anal. Chem.* **37**, 1351 (1965).
40. R. N. Adams, *Electrochemistry at Solid Electrodes*. Marcel Dekker, New York (1969).
41. R. J. Taylor and A. A. Humphrey, *Electroanal. Chem. Interfac. Electrochem.* **42**, 347 (1973).
42. C. A. Frysz, X. Shui and D. D. L. Chung (in prep.).